Journal of Physics: Conference Series **2687** (2024) 032033 doi:10.1088/1742-6596/2687/3/032033

Performance of laser patterned copper plasmonic photocathodes

M Martinez-Calderon[1]*, B Groussin[1], V Bjelland[1,2], E Chevallay[1], M Himmerlich[1], P Lorenz[3], B Marsh[1], H Neupert[1], R Rossel[1], W Wuensch[1], E Granados[1]*

[1] European Organization for Nuclear Research (CERN), 1211 Geneva, Switzerland
[2] Norwegian University of Science and Technology (NTNU), NO-7491 Trondheim, Norway
[3] Leibniz Institute of Surface Engineering (IOM), 04318 Leipzig, Germany

E-mail: miguel.martinez.calderon@cern.ch; eduardo.granados@cern.ch

Abstract. We study ultrafast laser surface nanopatterning as an alternative to improve the photo-emissive properties of metallic photocathodes. By tailoring the physical dimensions of these surface nanostructures, one can localize the optical field intensity and exploit plasmonic effects occurring in such nanostructures. As a result, this surface nanopatterning technique can become a great tool for improving metallic photocathodes photoemission behavior enabling their use for next generation high brightness electron sources. Our goal is to investigate such surface-plasmon assisted photoemission processes with a view on simplifying the photocathode production at CERN while extending the lifetime of existing photoinjectors. The performance of two different femtosecond laser nanopatterned plasmonic photocathodes was analyzed by measuring the quantum yield with a 65kV DC electron gun utilizing 266nm laser excitation generated by a nanosecond laser with 5ns pulse duration and 10Hz repetition rate. By comparing the electron emission of the copper surface nanostructured areas with that of a flat area, our results suggest quantum yield enhancements of up to a factor of 5.

1. Introduction

In the field of particle accelerator physics, the use of plasmonic nanostructures is extremely interesting and constitutes a pathway to more efficient photocathodes by optimizing the photoemission process either via increased light absorption or tailored electric field-enhancement. Plasmonic nanostructures have already been routinely utilized for electron beam production with specific phase space properties. Nanostars [1], nanorods [2], carbon nanotubes [3] and other multi-resonant particles [4] have shown exciting routes for spatiotemporal photocurrent control over femtosecond (fs) laser pulses thanks to frequency and polarization selective excitation of the fabricated plasmonic hot spots/nanotips. Even plasmonic lenses through bulls-eye designs have been demonstrated for spatiotemporal confinement of energetic electron pulses [5]. These electron emitters constitute a great way to generate ultrafast electron pulses with tailored properties and nanometer-scale density modulations of the electron beam which can be of great benefit in next-generation coherent X-FELs and ultrafast electron diffraction studies.

Most of these studies utilize IR fs-pulses and are tested for rather low peak current generation but are not a suitable option when a high average current needs to be extracted from the photocathode (need for µA-mA range). Advanced biomedical accelerator applications such as

Content from this work may be used under the terms of the Creative Commons Attribution 3.0 licence. Any further distribution of this work must maintain attribution to the author(s) and the title of the work, journal citation and DOI.
Published under licence by IOP Publishing Ltd

FLASH therapy for cancer treatment [6], energy recovery linacs [7], inverse Compton scattering sources [8] or new generation x-ray sources based on free electron lasers, rely on the use of photoinjectors as the electron beam source and require high peak and average current [9].

Photocathodes used nowadays for such applications are metals (such as Cu, Mg or Nb) or high quantum-efficiency positive-electron-affinity semiconductors like alkali-antimonides [10]. Metallic photocathodes tend to have relatively low QE (values in the 10^{-4} - 10^{-5} region when using UV-photons above work function) but are standardly the material of choice for most high peak brightness photoinjector guns due to their prompt response, low vacuum requirements, ruggedness and long lifetime. Therefore, new routes for enhancing metallic photocathodes QE will suppose a great advance for electron beam based applications.

In this work, we propose to use plasmonic nanostructures for enhancing directly the single-photon absorption photoemission process using UV laser pulses over metal's work function (the standard source of photocathode excitation in most of state-of-the-art electron accelerator facilities). By exploiting the field-enhancement generated from the interaction of the UV photons with resonant nanostructures, we are able to improve the measured quantum yield (QY) of two distinct plasmonic copper photocathodes with a DC-electron gun.

2. Surface nanopatterning

In order to generate such field-enhancements under UV laser irradiation, spherical nanoparticles (NPs) and/or periodic patterns with a sub-wavelength size are needed. However, it is known that the manufacturing of robust and reproducible structures in a size range smaller than 200 nm can be challenging [11].

To address this challenge, we take advantage of the direct ablation process induced by ultra-short pulsed lasers (same standard lasers used for photocathode irradiation) when the laser fluence is tuned slightly above the material's ablation threshold leading to different types of controllable size nanostructures.

The use of ultrafast lasers (fs and ps) for surface nanostructuring typically results into two main types of nanoscale features. First, the well-known ripple-like Laser Induced Periodical Surface Structures (LIPSS) with controllable sub-wavelength geometries depending on parameters such as irradiation wavelength, fluence, number of pulses or wavefront [12]. Second, the condensation of individual NPs and larger particle clusters covering the laser-treated surface arising from the rapid expansion and cooling of the ablation plume generated after the absorption of high-intensity ultra-short laser pulses [13, 14].

Interestingly, depending on the material and laser pulse duration, the use of fluences slightly above the material's ablation threshold can lead to a preferential generation of NPs with nanometric size and suppression of larger size clusters deposited at the surface which often arise at higher fluences [15, 16]. These NPs can present sizes in the range of few tens to hundreds of nanometers, which result to be perfect to tailor the plasmonic response of UV-illuminated photocathodes.

Sample photocathodes were fabricated utilizing two distinct fs-laser systems tuning the laser fluence to be slightly above the photocathodes ablation threshold aiming at generating soft nanopatterning. Figure 1 shows that the fabrication process led to a combination of LIPSS nanopatterns covered by numerous NPs.

The photocathode nanopatterned with a fs-laser with 800 nm wavelength, 150 fs pulse duration, 1 kHz frequency, focused spot size of 5.5 µm and scanned at 70 µm/s led to the nanopatterned areas showed in Fig. 1(a, c) and is identified as Cathode A. The photocathode nanopatterned with a fs-laser with 515 nm wavelength, 260 fs pulse duration 100 kHz frequency, focused spot size of 28 µm and scanned at 10 mm/s led to the nanopatterned areas showed in Fig. 1(b, d) and is identified as Cathode B. The resulting LIPSS nanopatterns presented a spatial periodicity of 550 nm and 380 nm respectively. However, alongside with the formation

of the nanoripples, NPs of considerably smaller size were observed in the SEM images. In this regard, the dominant NPs size measured over the nanopatterned areas presented an average diameter of 95 ±27nm and 64 ±17nm for each case, as shown in the insets of Fig. 1(c, d).

The insets of Fig. 1(a, b) show optical pictures of the final produced photocathodes and it is important to remark that in the case of Cathode A (inset Fig. 1a) only the central area of the photocathode was nanopatterned with the purpose of having flat areas to directly compare the effect of the nanostructures.

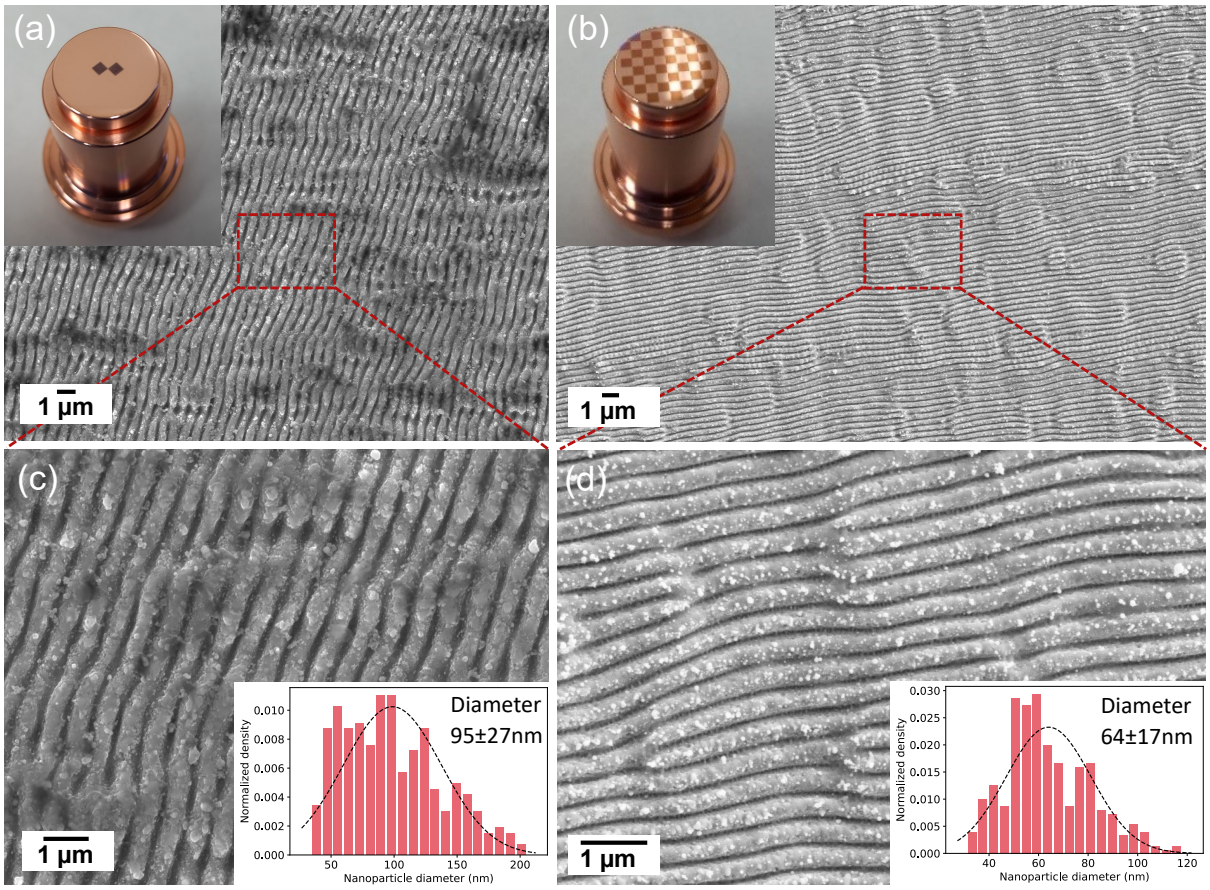

Figure 1. (a, b) SEM images of the nanopatterned areas with dimensions of 2x2mm, filled with LIPSS nanopatterns covered by NPs on Cathode A and B respectively. Inset pictures show the actual plugs prior introduction into the DC-GUN (c, d) Higher magnification SEM images of Cathode A and B respectively, with insets showing the measured NPs size distribution.

3. Surface composition analysis

An X-ray photoelectron spectroscopy (XPS) analysis of the surface composition of each photocathode was carried out inside the laser nanopatterned areas and in the non-treated areas (i.e. polished areas). The results presented in Table 1, indicate that the photocathode's surfaces presented residual Cs and Te traces which may have originated from the bake-out process used to achieve ultra-high vacuum conditions in the DC-GUN chamber housing the photocathodes reaching temperatures up to 250 degrees.

The difference in Cs and Te composition between polished and nano-patterned areas however is small, indicating that the residual deposition of Cs and Te was homogeneous along

the photocathodes surface and therefore allowing a relative comparison of the effect of the nanopatterns in the photoemission behavior during testing with the DC-GUN.

Table 1. Cathodes A and B surface composition at. % from XPS measurements

Cathode	Area	Cu	O	C	Te	Cs
A	structured	42.9	15.5	20.2	20.6	0.6
A	polished	44.1	4.8	21.9	28.1	1.0
B	structured	46.4	3.7	17.3	27.4	5.1
B	polished	48.8	3.1	15.5	28.2	4.4

4. Results

The photoemission experiments were conducted inside a DC electron gun with an online monitored constant base pressure of less than 10^{-11} mbar and a supplied voltage of 65 kV. The drive UV laser with λ= 266nm, 5 ns pulse duration and 10 Hz repetition rate was directed to the photocathodes surface via in-vacuum mirror with an incidence angle of 5 degrees, and focused to a gaussian beam spot size of approximately 2 mm diameter at the photocathodes surface. Finally, the electron beam current was online monitored by a wall-current monitor and a faraday cup.

For a complete QY assessment, we scanned the UV laser beam in x- and y- direction across the whole photocathodes surface and measured the generated current for different values of the UV laser pulse energy (online monitored by sampling the beam). The results are presented in Fig. 2.

As expected after the XPS analysis results, the measured QY for the polished copper areas was slightly higher than what has been reported for copper where the QY reported values are most of the times in the range of $1*10^{-5}$ - $5*10^{-5}$ for UV laser irradiation over the work function [17, 18]. Figure 2(a, c) shows that for polished copper areas in Cathode A the measured QY was $1*10^{-4}$. This result can be explained by the detected Cs and Te traces deposited during the heating of the DC-GUN preparation chamber.

In contrast, the QY measured from the nanostructured area of the same Cathode A was determined to be approximately $5*10^{-4}$, showing an almost 5 times enhancement clearly appreciated in the QY map presented in Fig. 2a. According to the XPS measurements, it seems unlikely that the QY increase comes from different Cs % measured in each area since the difference is very small. In addition, since the LIPSS nanopatterns periodicity (550 nm) is larger than the drive UV laser wavelength, they are not expected to provide any significant plasmonic field enhancement. Therefore, the main contributors for this enhancement are expected to be the previously characterized spherical nanoparticles with a measured diameter 95 $\pm$27nm.

Cathode B QY analysis is shown in Fig. 2(b, d). In this case, the whole photocathode area was nanopatterned with a checkerboard design that can be observed in the inset of Fig. 1b. The results for Cathode B show that the maximum measured QY ($2.5*10^{-3}$) is approximately 25 times higher than that of the polished areas of Cathode A. This promising result however needs to be taken with precaution since as shown in the XPS analysis, Cathode B presented a higher Cs content which might explain the higher QY increase. Apart from that, as shown in Fig. 1d, the NPs present in this cathode show a dominant size distribution with 64 $\pm$17nm diameter which can lead to higher local field-enhancements.

In the performed measurements, a local variation of the QY corresponding to the variation of polished or nanostructured regions could not be identified (see Fig. 2). The first possibility to

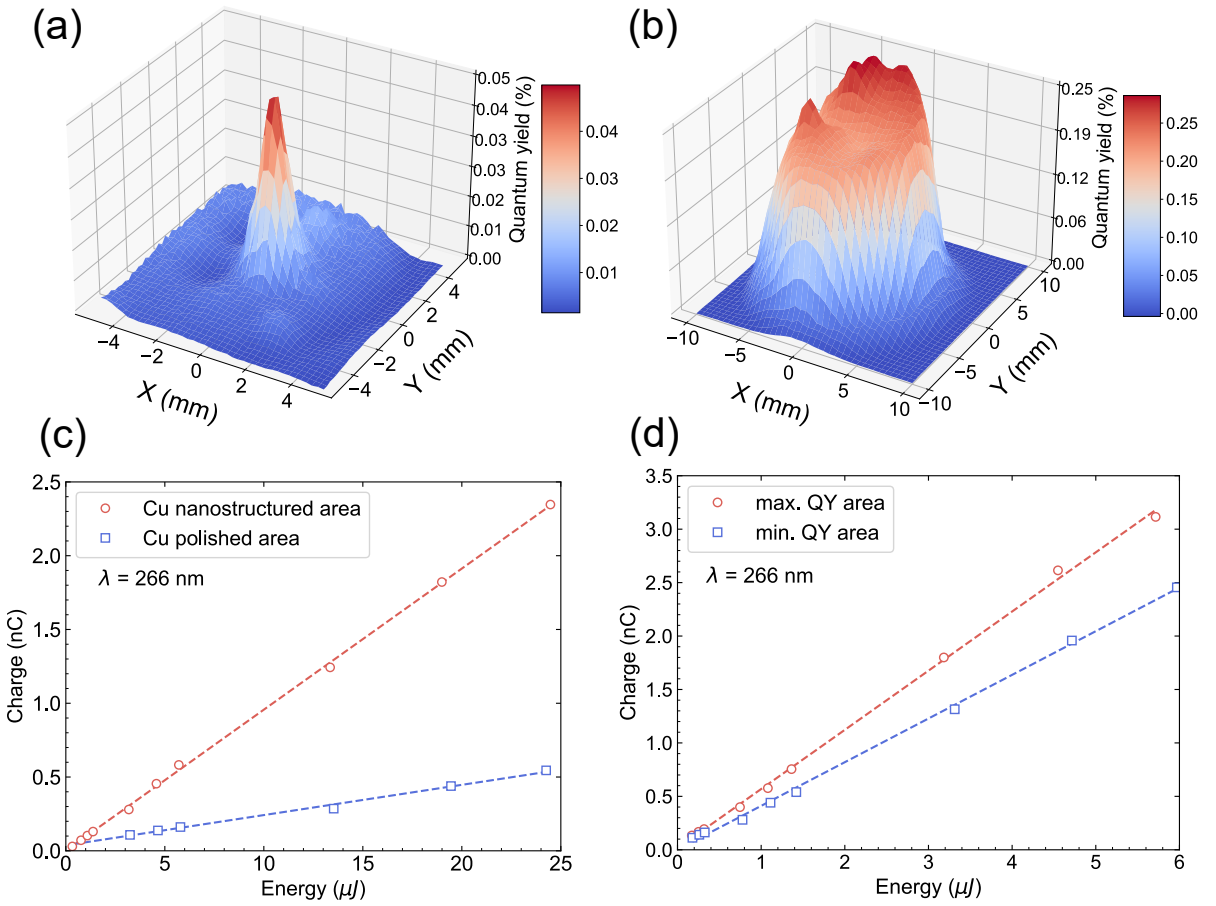

Figure 2. (a) Quantum yield map obtained for Cathode A using a pulse energy of 13.6μJ (b) Quantum yield map obtained for Cathode B using a pulse energy of 5.7μJ.(c) Electron beam charge as function of the UV laser energy delivered to Cathode A at the nanostructured area and at the polished area, corresponding to coordinates (0, 0) and (0,4) in the 3D map respectively. (d) Electron beam charge as function of the UV laser energy delivered to Cathode B at the point of maximum and minimum QY observed in the 3D map, corresponding to coordinates (0, 4.5) and (-2, 0) respectively.

explain this result is found in the UV laser spot size used in the experiments of approximately 2 mm diameter. Since the nanopatterned areas have a size of 2x2 mm, the laser spot was possibly too large to resolve these areas and therefore a possible local difference in electron emission is concealed in the measurement. Another possibility to explain why the nanopatterned areas were not resolved, might arise from the fact that commonly during the fs-laser nanopatterning process, debris particles are redeposited in the vicinity of the treated areas [19]. Therefore, if nm-size nanoparticles are present also in the polished areas near the nanopatterns they might contribute also to a field enhancement leading to the presented homogeneous QY maps. A post-mortem analysis will be conducted in the short future with Scanning Electron Microscopy to further investigate the nanoparticles distribution along the whole surface.

5. Conclusion

We present an innovative method for potentially improving metallic photocathodes performance using ultrafast laser (fs) surface nanopatterning with results showing an increase of at least 5 times in the measured QY after the first round of tests with this type of photocathodes at CERN. Further studies are required to address the exact contribution to the photo-current enhancement of the fabricated nanostructures as well as improvements in the experimental setup to avoid uncontrolled deposition of Cs or Te traces. These promising results show a new convenient way to enhance metallic photocathodes behavior under single-photon photoemission process which is the current standard in most of accelerator facilities. Moreover, nanopatterning a photocathode surface with the presented technique can be performed in most facilities directly with the typical UV ultrafast laser sources used to produce electron beams just by increasing the UV energy and focusing tighter the laser beam at the photocathode surface. Future experiments will include new nanopatterned photocathodes fabricated at CERN directly with UV ultrafast laser nanopatterning which will lead to smaller size LIPSS and nanoparticles.

References

[1] J. Pettine *et al.* 2020 Plasmonic nanostar photocathodes for optically-controlled directional currents *Nat Commun* **11** 1367
[2] R. G. Hobbs *et al.* 2014 High-Yield, Ultrafast, Surface Plasmon-Enhanced, Au Nanorod Optical Field Electron Emitter Arrays *ACS Nano* **8** (11) 11474-11482
[3] Mark E. Green *et al.* 2019 Bright and Ultrafast Photoelectron Emission from Aligned Single-Wall Carbon Nanotubes through Multiphoton Exciton Resonance *Nano Letters* **19** (1) 158-164
[4] W. Putnam *et al.* 2017 Optical-field-controlled photoemission from plasmonic nanoparticles *Nature Phys* **13** 335–339
[5] D. B. Durham *et al.* 2019 Plasmonic Lenses for Tunable Ultrafast Electron Emitters at the Nanoscale *Phys. Rev. Applied* **12** 054057
[6] MC. Vozenin*et al.* 2022 Towards clinical translation of FLASH radiotherapy *Nat Rev Clin Oncol* **19** 791–803
[7] C. Adolphsen *et al.* 2022 The Development of Energy-Recovery Linacs *arXiv preprint* arXiv:2207.02095
[8] K. Dupraz *et al.* 2020 The ThomX ICS source *Physics Open* **5** 100051
[9] N. A. Moody *et al.* 2018 Perspectives on Designer Photocathodes for X-ray Free-Electron Lasers: Influencing Emission Properties with Heterostructures and Nanoengineered Electronic States *Phys. Rev. Applied* **10** 047002
[10] J. Schaber *et al.* 2023 Review of photocathodes for electron beam sources in particle accelerators *J. Mater. Chem. C* **11** 3162-3179
[11] Hannah-Noa Barad *et al.* 2021 Large Area Patterning of Nanoparticles and Nanostructures: Current Status and Future Prospects *ACS Nano* **15** 4 5861–5875
[12] J. Bonse, *et al.* 2020 Maxwell Meets Marangoni—A Review of Theories on Laser-Induced Periodic Surface Structures *Laser and Photonics Reviews* **14** 2000215
[13] I. Saraeva *et al.* 2019 Effect of fs/ps laser pulsewidth on ablation of metals and silicon in air and liquids, and on their nanoparticle yields *Applied Surface Science* **470** 1018–1034
[14] M. Iqbal *et al.* 2020 The mechanism of laser-assisted generation of aluminum nanoparticles, their wettability and nonlinearity properties *Applied Surface Science* **527** 146702
[15] J. Perrière *et al.* 2007 Nanoparticle formation by femtosecond laser ablation *Journal of Physics D: Applied Physics* **40** 7069
[16] J.M. Guay *et al.* 2017 Laser-induced plasmonic colours on metals *Nat Commun* **8** 16095
[17] E. Prat *et al.* 2015 Measurements of copper and cesium telluride cathodes in a radio-frequency photoinjector *Phys. Rev. ST Accel. Beams* **18** 043401
[18] D.H. Dowell *et al.* 2010 Cathode R&D for future light sources *Nuclear Instruments and Methods in Physics Research Section A: Accelerators, Spectrometers, Detectors and Associated Equipment* **622** 3 685-697
[19] P. Balling *et al.* 2013 Femtosecond-laser ablation dynamics of dielectrics: basics and applications for thin films *Rep. Prog. Phys.* **76** 1–39